THE JOURNAL OF BIOLOGICAL CHEMISTRY VOL. 286, NO. 39, pp. 34007–34014, September 30, 2011

Structural Contribution of C-terminal Segments of NuoL (ND5) and NuoM (ND4) Subunits of Complex I from *Escherichia coli*[*] [S]

Received for publication, May 14, 2011, and in revised form, July 12, 2011 Published, JBC Papers in Press, August 11, 2011, DOI 10.1074/jbc.M111.260968

Jesus Torres-Bacete, Prem Kumar Sinha, Akemi Matsuno-Yagi, and Takao Yagi[1]

From the Department of Molecular and Experimental Medicine, MEM-256, The Scripps Research Institute, La Jolla, California 92037

The proton-translocating NADH-quinone oxidoreductase (complex I/NDH-1) is a multisubunit enzymatic complex. It has a characteristic L-shaped form with two domains, a hydrophilic peripheral domain and a hydrophobic membrane domain. The membrane domain contains three antiporter-like subunits (NuoL, NuoM, and NuoN, *Escherichia coli* naming) that are considered to be involved in the proton translocation. Deletion of either NuoL or NuoM resulted in an incomplete assembly of NDH-1 and a total loss of the NADH-quinone oxidoreductase activity. We have truncated the C terminus segments of NuoM and NuoL by introducing STOP codons at different locations using site-directed mutagenesis of chromosomal DNA. Our results suggest an important structural role for the C-terminal segments of both subunits. The data further advocate that the elimination of the last transmembrane helix (TM14) of NuoM and the TM16 (at least C-terminal seven residues) or together with the HL helix and the TM15 of the NuoL subunit lead to reduced stability of the membrane arm and therefore of the whole NDH-1 complex. A region of NuoL critical for stability of NDH-1 architecture has been discussed.

The proton-translocating NADH-quinone oxidoreductase (complex I,[2] EC 1.6.5.3) is the first enzyme of the respiratory chain in most eukaryotic cells. Complex I catalyzes the electron transfer from NADH to quinone, which is linked to the translocation of four protons through the inner mitochondrial membrane. This enzymatic complex, made up of 45 different polypeptides, is one of the largest enzymes of the respiratory chain, with a molecular mass of ~1000 kDa (1, 2). The physiological importance of complex I is highlighted by the fact that this enzyme is the principal source of reactive oxygen species in mitochondria and that its deficiencies have been shown to be the origin of many human neurodegenerative diseases (3–5). The bacterial enzyme (NDH-1) is composed only of 14 subunits with a molecular mass of 500 kDa (6, 7). All subunits of NDH-1 are homologous to the 14 subunits that constitute the core of the mitochondrial complex I (8, 9). Both eukaryotic complex I and prokaryotic NDH-1 have a characteristic L-shaped form with two clearly defined domains, a hydrophilic peripheral arm projected into the mitochondrial matrix/bacterial cytoplasm, and a hydrophobic arm embedded in the inner mitochondrial/cytoplasmic membrane (10). The hydrophilic domain houses all of the cofactors that participate in the electron transfer from NADH to quinone (11–16).

The membrane domain of NDH-1 is composed of seven subunits (named NuoA, NuoH, NuoJ, NuoK, NuoL, NuoM, and NuoN in *Escherichia coli*), which are all homologues of the mammalian mitochondrial encoded subunits ND3, ND1, ND6, ND4L, ND5, ND4, and ND2, respectively. Recently, Sazanov's group (7) reported the three-dimensional structural model of the transmembrane segment of *E. coli* NDH-1 at 3.9 Å resolution and of the whole structure of *Thermus thermophilus* at 4.5 Å. These structures confirmed the membrane distribution of the hydrophobic subunits that were previously outlined by biochemical methods (10, 17–20), in which the hydrophobic subunits NuoA, -H, -J, -K, and -N are located close to the peripheral arm, whereas the NuoM and NuoL subunits are present at the end of the membrane arm, in its distal part. The NuoA, -K, and -J subunits form a bundle and are in contact with the hydrophilic domain subunits NuoCD and NuoB, possibly making a quinone binding pocket at the interface between the hydrophilic and the hydrophobic domain. The structure of the hydrophobic domain revealed a common topology for the NuoL, NuoN, and NuoM, wherein these subunits were composed of 12 continuous transmembrane (TM) helices and two discontinuous TM helices. The longer subunit NuoL, however, possesses two extra TM helices. One of the most interesting findings from this structure is that these two extra helices are connected by a long amphipathic α-helix (110 Å in case of *E. coli*), the HL helix, which is spanning from NuoL, through NuoM, to NuoN, making a bridge among these subunits (7).

The distal location of the antiporter-like subunits, NuoL, NuoM, and NuoN from the electron transfer pathway strongly suggested a long range conformational change as essential part of the energy-coupling mechanism of complex I/NDH-1 (indi-

[*] This work was supported by National Institutes of Health Grant R01GM033712 from USPHS (to T. Y. and A. M.-Y.).

[S] The on-line version of this article (available at http://www.jbc.org) contains supplemental Table 1, Figs. 1 and 2, and additional references.

[1] To whom correspondence should be addressed: The Scripps Research Institute, Dept. of Molecular and Experimental Medicine, 10550 N. Torrey Pines Rd., MEM256, La Jolla, CA 92037. Fax: 858-784-2054; E-mail: yagi@scripps.edu.

[2] The abbreviations used are: complex I, mitochondrial proton-translocating NADH-quinone oxidoreductase; NDH-1, bacterial proton-translocating NADH-quinone oxidoreductase; ctNuoL, C-terminus truncated NuoL; ctNuoM, C-terminus truncated NuoM; DB, 2,3-dimethoxy-5-methyl-6-decyl-1,4-benzoquinone; dNADH, reduced nicotinamide hypoxanthine dinucleotide; oxonol VI, bis-(3-propyl-5-oxoisoxazol-4-yl)pentamethine oxonol; ACMA, 9-amino-6-chloro-2-methoxyacridine; FCCP, carbonyl cyanide-*p*-trifluoromethoxy-phenylhydrazone; TM, transmembrane segment(s); BN-PAGE, blue native PAGE.

rect coupling) (8, 21–27). Based on the three-dimensional structure, Sazanov and co-workers (7) have hypothesized that the HL helix of NuoL can work in a piston-like mechanism, driving the conformational changes along the antiporter-like subunits.

In the present work, using *E. coli* NDH-1, we attempted to clarify the structural role of the C-terminal segments of NuoL and NuoM that are most distantly located from the peripheral domain. Primary sequence comparison of the NuoL extra stretch or the NuoM C-terminal region among diverse organisms indicated that amino acid residues are barely conserved in these regions. Therefore, conventional mutation approach (mutation of the conserved residues) does not seem to be useful. Therefore, we created truncation mutants by introducing stop codons directly on the *nuoL* and *nuoM* genes in the chromosomal NDH-1 operon by site-directed mutagenesis and investigated their effects on the architecture and enzymatic activities of NDH-1.

Recently, study of the NuoL extra stretch has been published by Steimle *et al.* (28). The results by Steimle *et al.* (28) were significantly different from this work. Possible causable factors leading to these differences were also discussed.

EXPERIMENTAL PROCEDURES

Materials—PCR product, DNA gel extraction, and plasmid purification kits were from Qiagen (Valencia, CA). The pGEM®-T Easy Vector System was from Promega (Madison, WI). The site-directed mutagenesis kit (QuikChange® II XL kit) and the Herculase® Enhanced DNA polymerase were from Stratagene (Cedar Creek, TX). The pKO3 vector was a generous gift from Dr. George M. Church (Harvard Medical School, Boston, MA). The endonucleases were from New England Biolabs (Beverly, MA). *p*-Nitroblue tetrazolium was from EMD Biosciences (La Jolla, CA). All other chemicals including dNADH, NADH, and antibiotics were from Sigma-Aldrich. The antibodies against *E. coli* NDH-1 subunits NuoB, NuoCD, NuoE, NuoF, NuoG, NuoI, NuoK, NuoM, and NuoL were obtained previously in our laboratory (29–31). Primer sequences are summarized in supplemental Table 1. *E. coli* MC4100 (F^-, araD139, Δ(arg F-lac)U169, ptsF25, relA1, flb5301, rpsL 150.λ^-) was used to generate *nuoL* and *nuoM* site-specific mutations.

Preparation of NuoL and NuoM Knock-out and Mutagenesis of nuoL and nuoM Gene in E. coli Chromosome—The NuoL knock-out (NuoL-KO) and the C terminus-truncated NuoL (ctNuoL) mutants were generated by employing the pKO3 system according to the method described by Link *et al.* (32) and Nakamaru-Ogiso *et al.* (25) with minor modifications. In brief, an *E. coli* NuoL-KO was constructed by replacement of the *nuoL* gene in the NDH-1 operon by spectinomycin using the pKO3 system. In parallel, a DNA fragment that includes the *nuoL* gene together with a 1-kb upstream and 1-kb downstream DNA segments from *E. coli* DH5α was cloned in the pGEM®-T Easy Vector system, generating pGEM/*nuoL*. pGEM/*nuoL* was used as template to obtain the *nuoL*-STOP mutants and the *nuoL*-ΔV519-K581 mutant. The *nuoL* mutants were subcloned into the pKO3 vector generating the pKO3/*nuoL*(STOP mutants) or pKO3/*nuoL*(ΔV519-K581). The pKO3/*nuoL*-(STOP mutants) and the pKO3/*nuoL*(ΔV519-K581) plasmids were used to replace the spectinomycin gene in *E. coli nuoL-KO* by recombination. The strategy used to obtain the NuoM knock-out (NuoM-KO) and the C terminus truncated NuoM (ctNuoM) mutants were the same as we reported previously in Torres-Bacete *et al.* (31). All mutations were confirmed by DNA sequencing.

Growth and Membrane Preparation of E. coli Mutants—*E. coli* ctNuoL and ctNuoM mutants were grown and the inverted membrane vesicles were prepared according to the method described previously in our laboratory (31, 33–36). In summary, the *E. coli* cells were grown in Terrific Broth medium at 37 °C until A_{600} of 2. Then, the cells were harvested and frozen at −80 °C. The cells were thawed and resuspended at 10% (w/v) in buffer A (10 mM Tris-HCl (pH 7.0), 1 mM EDTA, 1 mM dithiothreitol, 1 mM phenylmethanesulfonyl fluoride, and 15% glycerol). The cell suspension was sonicated twice (15 s) and passed twice through a French press (15,000 psi). The cell debris was removed by centrifugation (23,400 × *g* for 10 min). The supernatant was centrifuged again (256,600 × *g* for 30 min), and the membrane-rich pellet was resuspended in buffer A, frozen in liquid nitrogen, and stored at −80 °C before use.

Immunoblots and Blue Native Electrophoresis—The content of the NDH-1 subunits were analyzed by Western blot using antibodies against NuoB, NuoCD, NuoE, NuoF, NuoG, NuoI, NuoK, NuoL, and NuoM subunits. For the production of the NuoL and NuoM antibodies, we selected the peptides H^{357}HEQNIFKMGGLRKS^{371} (the loop between TM11 and TM12 in NuoL) and F^{205}NYEELLNTPMS^{216} (the loop between TM6 and TM7 in NuoM), respectively (25, 31). Blue native PAGE was performed according to the method described previously (35). The assembly of NDH-1 was examined by immunoblotting using anti-NuoL and NuoCD antibodies and NADH dehydrogenase activity staining (25, 34).

Activity Analysis—The measurements of the electron transfer activities by the NDH-1 ctNuoL and ctNuoM mutants were performed using dNADH as substrate. The enzymatic reactions were conducted at 30 °C in a SLM DW-2000 spectrophotometer according to the methods described previously (37). In brief, the dNADH-$K_3Fe(CN)_6$ reductase activity was performed using 80 μg of protein/ml of membrane samples in 10 mM potassium phosphate (pH 7.0), 1 mM EDTA containing 10 mM KCN, and 1 mM $K_3Fe(CN)_6$. The reaction was started by the addition of 150 μM dNADH. The absorbance change was monitored at 420 nm. The dNADH-DB reductase activity was conducted in a similar way using 50 μM DB as the electron acceptor instead of $K_3Fe(CN)_6$. The absorbance change was followed at 340 nm. The dNADH oxidase activity was performed under the same conditions except that neither KCN nor DB were added. Extinction coefficients of $\epsilon_{420} = 1.00\ mM^{-1}\ cm^{-1}$ for $K_3Fe(CN)_6$ and $\epsilon_{340} = 6.22\ mM^{-1}\ cm^{-1}$ for dNADH were used for the activity calculations.

We observed that despite the complete absence of dNADH oxidase and dNADH-DB reductase activity the NuoL-KO and NuoM-KO mutants still showed residual (~30%) dNADH-$K_3Fe(CN)_6$ reductase activity. It is known that dNADH-$K_3Fe(CN)_6$ reductase activity of NDH-1 needs at least NuoF (the NADH-binding subunit) and NuoE (38). The NuoL-KO

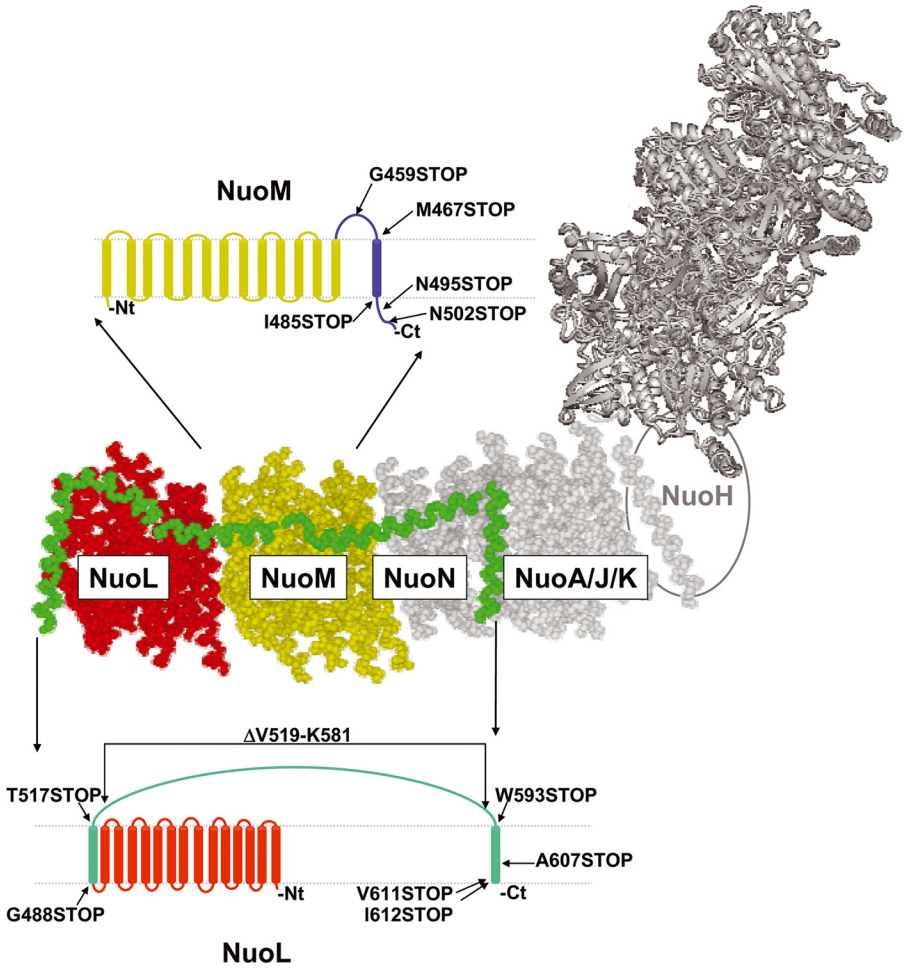

FIGURE 1. **A schematic representation of the membrane domain of *E. coli* fused with the peripheral domain of *T. thermophilus* (in *gray*).** The NuoL subunit is shown in *red*, and the HL helix, TM15 and TM16 are highlighted in *green*. The NuoM subunit is colored *gold*. The positions at which NuoL or NuoM were truncated are marked in two separate schematic representations of both subunits. Three-dimensional structures were taken from Protein Data Bank codes 3M9C (*E. coli*) and 3IAS (*T. thermophilus*).

mutant lacks NuoF and NuoE in the membranes and the NuoM-KO mutant does not house NuoF. In addition, similar activity was observed in a NuoF knock-out mutant. This is most likely a diaphorase activity unrelated to NDH-1. Therefore, the values obtained for the NuoL-KO and NuoM-KO mutants were subtracted as a background activity from the activity values of the wild type and the different mutants analyzed.

The generation of membrane potential for the ctNuoL and ctNuoM mutants was assayed using 0.33 mg of protein/ml of membrane vesicles in 50 mM MOPS (pH 7.3), 10 mM $MgCl_2$, 50 mM KCl, and 2 μM oxonol VI as described previously (33, 39). The reaction was started by addition of 0.2 mM dNADH, and the absorbance changes at 630–603 nm were recorded. The proton ionophore FCCP (2 μM) was added to uncouple the reaction. The NDH-1 proton pump activity was followed by ACMA fluorescence quenching (40). 50 μg of protein/ml of membrane vesicles was used for the assay, whereas 200 μM dNADH was used as substrate.

Other Analytical Procedures—Protein concentrations were determined by the BCA protein assay kit (Pierce) with bovine serum albumin as standard, according to the manufacturer's instructions. Any variations from the procedures and details are described in the figure legends.

RESULTS

Mutant Constructs for Subunits NuoL/ND5 and NuoM/ND4—NuoL and NuoM are two of the most well conserved membrane subunits in NDH-1/complex I from bacteria to mammals (see supplemental Figs. 1 and 2). Both NuoL and NuoM subunits share a similar secondary structure (7), except that the longer NuoL subunit possesses two extra TM helices, TM15 and TM16, connected by a long amphipathic helix (HL). This TM15-HL-TM16 C-terminal region displays low sequence homology among the diverse organisms. As described in the Introduction, we investigated structural role of the extra stretch of ctNuoL and C-terminal region of NuoM by using truncated mutation technique. Fig. 1 shows the locations at which the stop codons were introduced. In the NuoL subunit, these positions are Gly^{488} (NuoL was truncated at the beginning of the TM15), Thr^{517} (truncation at the beginning of the HL helix), Trp^{593} (truncation toward the end of the HL helix), Ala^{607} (truncation in the middle of the TM16), Val^{611} (truncated three residues before the C terminus of NuoL) and Leu^{612} (truncated two residues before the C terminus; last residue of the TM16). We also constructed a NuoL mutant in which the complete HL helix was lacking, whereas the TM helices 15 and 16 were intact

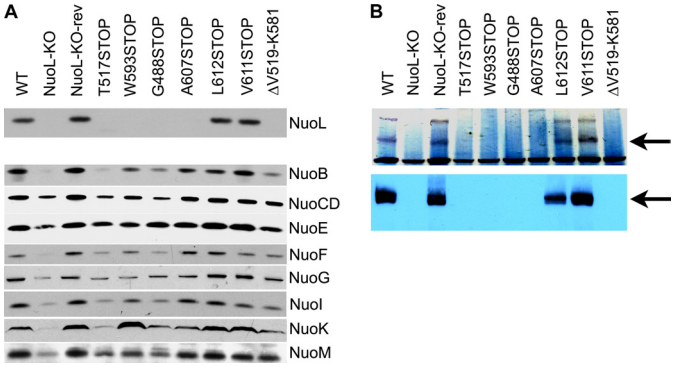

FIGURE 2. *A*, immunoblotting of membrane preparations from the ctNuoL mutants. Antibodies against the NuoL, NuoB, NuoCD, NuoE, NuoF, NuoG, NuoI, NuoK, and NuoM subunits were used. 15 μg of protein per lane was loaded on a 4–20% Tris-glycine gel (Invitrogen). The secondary antibody used was goat anti-rabbit IgG horseradish peroxidase conjugate (GE Healthcare). *B*, BN-PAGE of membrane preparations of the ctNuoL mutants. *Top row*, NADH dehydrogenase activity staining; *bottom row*, immunoblotting using antibodies against the NuoL subunit. The *arrows* show the location of the NDH-1 band. For activity staining, the gels were incubated for 1 h with 2.5 μg/ml *p*-nitroblue tetrazolium and 0.15 mM NADH in 2 mM Tris buffer (pH 7.5) at 37 °C. The reaction was stopped by 7% acetic acid. For immunoblotting, after the BN-PAGE, *E. coli* membrane proteins were electrotransferred onto nitrocellulose membranes. Affinity-purified NuoL antibody was used as the primary antibody. The secondary antibody used was goat anti-rabbit IgG horseradish peroxidase conjugate (GE Healthcare).

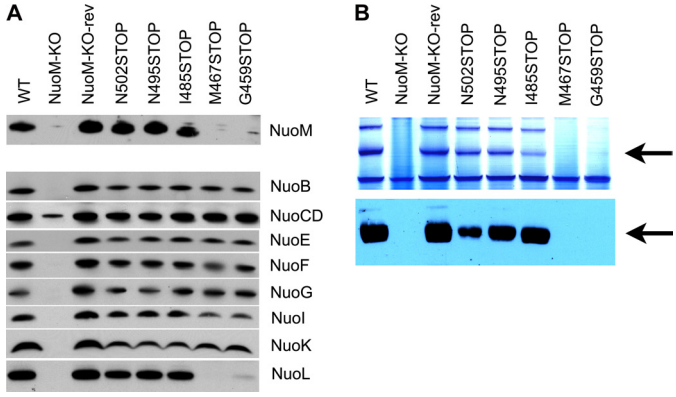

FIGURE 3. *A*, immunoblotting of membrane preparations from the ctNuoM mutants. Antibodies against the NuoM, NuoB, NuoCD, NuoE, NuoF, NuoG, NuoI, NuoK, and NuoL subunits were used. 15 μg of protein per lane was loaded on a 4–20% Tris-glycine gel (for details, see Fig. 2*A*). *B*, BN-PAGE of membrane preparations of the ctNuoM mutants. *Top row*, NADH dehydrogenase activity staining; *Bottom row*, Immunoblotting using antibodies against the NuoL subunit. The *arrows* show the location of the NDH-1 band (for details, see Fig. 2*B*).

(ΔV519-K581, Fig. 1). In the NuoM subunit, the positions at which the stop codons were introduced are Asn^{502} and Asn^{495} (truncation in the middle of the periplasmic C-terminal segment at two different positions), Ile^{485} (in which the periplasmic C-terminal segment was eliminated), Met^{467} (in which TM14 was eliminated), and Gly^{459} (truncation in the middle of the cytoplasmic loop that connects TM13 and TM14).

Assembly and Subunit Contents of ctNuoL and ctNuoM Mutants—We studied the effect of the C terminus truncation mutants, ctNuoL and ctNuoM, on the subunit contents and architecture of NDH-1 by Western blotting and BN-PAGE. We used antibodies raised against the NuoL and NuoM subunits, and another seven NDH-1 subunits: the peripheral subunits NuoB, NuoCD, NuoE, NuoF, NuoG, NuoI, and the membrane subunit NuoK. The results are exhibited in Figs. 2 and 3. As expected, membrane vesicles from the NuoL knock-out (NuoL-KO) and NuoM knock-out (NuoM-KO) mutants totally lacked the NuoL and NuoM subunit, respectively. The contents of other NDH-1 subunits were also affected. NuoCD was detected in both deletion mutants, albeit at a lower level. However, other subunits examined were either significantly diminished (NuoL-KO) or not discernible (NuoM-KO). It is important to note that the NuoL-KO-rev and NuoM-KO-rev mutants showed similar protein levels for all the subunits analyzed when compared with the wild type. As shown in Fig. 2*A*, in the C terminus truncation mutants of NuoL (G488STOP, T517STOP, W593STOP, and A607STOP), the amount of NuoL was either greatly reduced or too low to detect. As expected, membranes of these mutants also showed reduced contents of other NDH-1 subunits. The result for the mutant ΔV519-K581 was similar to those of the aforementioned truncation mutants. In contrast, two truncation mutants V611STOP and L612STOP retained a normal level of NuoL together with the other subunits. All of the truncated NuoL mutants showed significant amounts of NuoM in the membranes. As shown in Fig. 3*A*, in the case of NuoM truncation mutants lacking the TM14 (G459STOP and M467STOP), neither NuoM nor NuoL was detectable. Interestingly, the other NDH-1 subunits analyzed for the above two mutants showed contents mostly comparable with the wild type. The rest of the ctNuoM mutants constructed displayed NDH-1 subunits content at a level similar to the wild type.

We analyzed the membranes of the ctNuoL mutants by BN-PAGE. As shown in Fig. 2*B*, no NDH-1 assembly was detected in the membranes of the NuoL-KO mutant either by activity staining or by immunoblot using antibodies against the NuoCD subunit (data not shown). Here again, the revertant showed normal assembly of NDH-1 like the wild type. Among the ctNuoL mutants constructed, only the ctNuoL-V611STOP and -L612STOP mutants showed positive activity staining in the BN-PAGE comparable with the wild type. In agreement with the activity staining results, no NDH-1 assembly was detected by immunoblotting in the ctNuoL-G488STOP, -T517STOP, -W593STOP, -A607STOP, and -ΔV519-K581 mutants. The correct assembly of NDH-1 in the ctNuoM mutants was analyzed by BN-PAGE (Fig. 3*B*). As expected from the immunoblot experiments, no NDH-1 assembly was detected in the ctNuoM mutants in which the TM14 was truncated (ctNuoM-G459STOP and -M467STOP).

Effect of NuoL and NuoM Truncations on NDH-1 Electron Transfer Activities—*E. coli* contains the alternative NADH-quinone oxidoreductase (or NDH-2) in addition to NDH-1. Because NDH-1 can use dNADH as substrate, whereas NDH-2 cannot, all enzymatic assays were performed using dNADH as the substrate to eliminate contribution from NDH-2 (41). We measured the electron transfer activities of NDH-1 in membrane vesicles obtained from *E. coli* MC4100 wild type and the ctNuoL and ctNuoM mutants (Table 1). The electron transfer activities assayed were the dNADH-$K_3Fe(CN)_6$ oxidoreductase, dNADH oxidase, and dNADH-DB oxidoreductase of NDH-1.

The dNADH-$K_3Fe(CN)_6$ reductase activity, derived from the NuoF+NuoE subunits (38), has been used as a measure for the

TABLE 1
Enzymatic activities of the ctNuoL and ctNuoM mutants of *E. coli* NDH-1

Mutant	dNADH-O_2[a]	dNADH-DB[b]	dNADH-$K_3Fe(CN)_6$[c]
	%	%	%
WT	100 ± 6.0	100 ± 8.0	100 ± 4.7
NuoL-KO-rev	102 ± 2.7	86 ± 5.1	100 ± 5.9
NuoM-KO-rev	113 ± 4.4	95 ± 14.0	106 ± 6.1
ctNuoL-G488STOP	2 ± 0.9	2 ± 0.3	18 ± 2.3
ctNuoL-T517STOP	1 ± 1.0	2 ± 1.2	27 ± 3.5
ctNuoL-W593STOP	1 ± 0.4	3 ± 0.7	27 ± 2.9
ctNuoL-A607STOP	4 ± 1.9	2 ± 0.3	20 ± 1.9
ctNuoL-V611STOP	66 ± 6.7	67 ± 3.2	80 ± 5.8
ctNuoL-L612STOP	89 ± 11.0	73 ± 5.7	91 ± 3.5
ctNuoL-ΔV519-K581	1 ± 0.4	1 ± 2.0	30 ± 4.7
ctNuoM-G459STOP	9 ± 1.1	9 ± 0.6	33 ± 1.2
ctNuoM-M467STOP	2 ± 0.6	1 ± 0.3	33 ± 0.6
ctNuoM-I485STOP	64 ± 2.2	60 ± 3.8	67 ± 5.6
ctNuoM-N495STOP	77 ± 0.8	67 ± 6.8	75 ± 4.5
ctNuoM-N502STOP	81 ± 9.4	79 ± 2.3	75 ± 0.6

[a] Percentage of dNADH-O_2 reductase activity (100% activity of WT was 0.61 μmol dNADH/mg protein/min).
[b] Percentage of dNADH-DB reductase activity (100% activity of WT was 0.69 μmol dNADH/mg protein/min).
[c] Percentage of dNADH-$K_3Fe(CN)_6$ reductase activity (100% activity of WT was 1.5 μmol $K_3Fe(CN)_6$/mg protein/min).

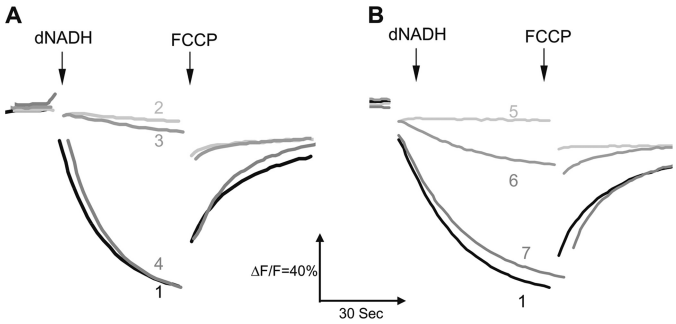

FIGURE 4. **Effect of the ctNuoL and ctNuoM mutations on the ΔpH coupled to dNADH oxidation in *E. coli* membrane vesicles (50 μg of protein/ml).** The proton translocation activity was monitored by the quenching of ACMA at room temperature. An excitation wavelength of 410 nm and emission wavelength of 480 nm was used. At the time indicated by the *arrows*, 0.2 mM of dNADH or 10 μM FCCP was added. Assay buffer consisted of the following: 50 mM MOPS (pH 7.3), 10 mM $MgCl_2$, 50 mM KCl, and 2 μM ACMA. *A*, ctNuoL mutants: *curve 1*, wild type; *curve 2*, NuoL-KO; *curve 3*, ctNuoL-G488STOP, -T517STOP, -W593STOP, -A607STOP, and -ΔV519-K581; *curve 4*, ctNuoL-V611STOP and -L612STOP. *B*, ctNuoM mutants. *Curve 1*, wild type and ctNuoM-N495STOP and -N502STOP; *curve 5*, NuoM-KO and ctNuoM-M467STOP; *curve 6*, ctNuoM-G459STOP; *curve 7*, ctNuoM-I485STOP.

correct assembly of the peripheral arm of NDH-1. This activity was significantly affected in the mutants where the assembly of the whole NDH-1 complex was compromised. As seen in Table 1, the ctNuoL-G488STOP, -T517STOP, and ΔV519-K581 mutants that lack the HL helix, showed only ~20–30% of the dNADH-$K_3Fe(CN)_6$ reductase activity when compared with the wild type. Similar results were obtained in case of the mutants with the HL helix intact but in which TM16 was totally or partially eliminated ctNuoL-W593STOP and -A607STOP. The dNADH-$K_3Fe(CN)_6$ reductase activity was found to be similar to the wild type (80 and 91%, respectively) only when NuoL was truncated at the last two or three residues prior to the C terminus (ctNuoL-V611STOP and -L612STOP). These results highlight not only the importance of the HL helix in keeping the structure of the membrane arm but also the role of the TM16 for the correct anchorage of the intact structure.

In accordance with the results of dNADH-$K_3Fe(CN)_6$ reductase activity, the ctNuoL mutants lacking the HL helix and/or the TM16 did not show energy-coupled NDH-1 activities (dNADH oxidase and dNADH-DB reductase) (Table 1). Once again, only the ctNuoL-V611STOP and -L612STOP mutants, which showed a correct NDH-1 assembly, had energy-coupled activities similar to those of the wild type (~65 and ~85%, respectively).

Akin to the results observed for the ctNuoL mutants, the ctNuoM mutants lacking the last TM helix TM14 (ctNuoM-G459STOP and -M467STOP) showed a diminished dNADH-$K_3Fe(CN)_6$ reductase activity (30%) as compared with the wild type (Table 1). In the case of ctNuoM mutants in which the periplasmic C-terminal segment was truncated (ctNuoM-I485STOP, -N495STOP, and -N502STOP), the dNADH-$K_3Fe(CN)_6$ reductase activity decreased by ~30–25% of the wild type. The electron transfer activities of these mutants were found to be affected in a similar manner.

We have measured the proton translocation activity in inverted membrane vesicles of the ctNuoL and ctNuoM mutants. The analysis of the formation of a proton gradient (ΔpH, acid inside) was performed using ACMA as a fluorescence indicator. As seen in Fig. 4, membrane vesicles from the wild type showed a maximum quenching after the addition of dNADH. The signal was completely restored when the ionophore FCCP was added. In contrast, the NuoL-KO mutant did not show any change in the ACMA signal after the addition of dNADH, indicating the absence of proton pump activity (Fig. 4*A*). A similar result was observed for the NuoM-KO mutant (Fig. 4*B*). Membrane vesicles of the ctNuoL-G488STOP, -T517STOP, -W593STOP, -A607STOP, and -ΔV519-K581 mutants did not show any proton pump activity. Only in the ctNuoL-V611STOP and -L612STOP mutants was the proton pump activity found to be unaffected.

In the case of the ctNuoM mutant, two different results were observed when the last TM helix was eliminated. The ctNuoM-M467STOP did not show any proton pump activity; however, interestingly the ctNuoM-G459STOP mutant retained ~20% of the proton pump activity as compared with the wild type (Fig. 4*B*). On the other hand the ctNuoM-I485STOP, -N495STOP, and -N502STOP mutants showed activity similar to the wild type.

In conjunction with the proton pump activity, we analyzed the generation of membrane potential (ΔΨ) in the membrane vesicles of the ctNuoL mutants using oxonol VI as the reporter (Fig. 5). Membrane vesicles of the wild type showed a maximum ΔΨ after the addition of dNADH, and FCCP totally abolished the ΔΨ. No ΔΨ was generated in the case of NuoL-KO and NuoM-KO mutants. Similar results were obtained for the ctNuoL mutants lacking the HL helix and/or the transmembrane α-helix 16. Interestingly, a minor ΔΨ was observed in the ctNuoL-A607STOP mutant (Fig. 5*E*). In agreement with the results on ΔpH, the mutants ctNuoL-V611STOP and -L612STOP showed a ΔΨ generation comparable with that of the wild type. In the case of the ctNuoM mutants that lacked the last TM helix, ΔΨ was almost null (Fig. 5, *F* and *G*), and ctNuoM-I485STOP, -N495STOP, and -N502STOP showed a ΔΨ comparable with the wild type.

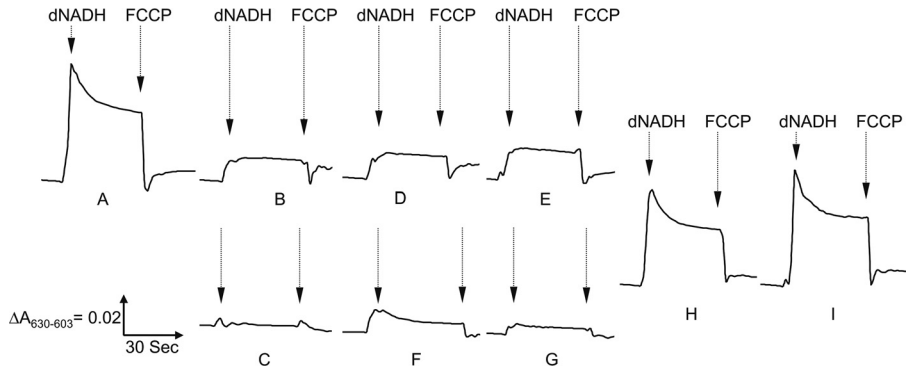

FIGURE 5. **Detection of the membrane potential (ΔΨ) generated by dNADH oxidation in the ctNuoL and ctNuoM mutants.** The membrane potential (ΔΨ) was monitored by the absorbance changes of oxonol VI at 630 – 603 nm at 37 °C. The assay mixture includes membrane samples (0.33 mg of protein/ml) in 50 mM MOPS (pH 7.3), 10 mM $MgCl_2$, 50 mM KCl and 2 μM oxonol VI. At the time indicated by the *arrows*, 0.2 mM dNADH or 2 μM FCCP was added. *A*, wild type; *B*, NuoL-KO; *C*, NuoM-KO; *D*, ctNuoL-G488STOP, -T517STOP, -W593STOP, and -ΔV519-K581; *E*, ctNuoL-A607STOP; *F*, ctNuoM-G459STOP; *G*, ctNuoM-M467STOP; *H*, ctNuoL-V611STOP and ctNuoM-I485STOP; *I*, ctNuoL-L612STOP and ctNuoM-N495STOP and -N502STOP.

DISCUSSION

Our current and earlier results indicated that deletion of a subunit in *E. coli* NDH-1 can lead to incomplete assembly of the complex. When subunit NuoA (35), NuoCD (36), NuoH (42), NuoJ (33), NuoK (34), NuoM (31), or NuoL was individually deleted, the amount of other subunits were reduced to various extents. Mutants lacking NuoCD or NuoH seemed to be most drastically affected with nearly a total loss of NDH-1 assembly, which may agree with their location in the core of the complex (36). The distal location of antiporter-like subunits NuoM and NuoL (7, 43) might suggest that their removal would not affect the activity of the peripheral domain. However, our results with the deletion mutants demonstrated a complete absence of the NADH-quinone reductase activity if either was absent (25, 44). The null activity of these mutants could be explained by the incorrect NDH-1 assembly and the reduced levels of other subunits examined. In fact, NuoL-KO mutant retained only two subunits NuoCD and NuoE in the membrane. In the case of NuoM-KO mutant only, the NuoCD subunit was detected in the membranes. Nakamaru-Ogiso *et al.* (25) described the presence of small inactive NDH-1 subcomplexes when the NuoL-KO membrane was analyzed by BN-PAGE. Quite similar results were reported by Dupuis *et al.* (45, 46) who described a deficit of NDH-1 activity and assembly in membranes vesicles of the NuoL knock-out mutant from *Rhodobacter capsulatus*. Furthermore, it was described that the deletion of the homologue MrpA subunit from the Na^+/H^+ antiporter from *Bacillus subtilis* results into complete loss of activity (47, 48). Interestingly, this loss of activity could be compensated by the homologue subunit NuoL from *E. coli* (49). These observations are not unique to bacterial enzymes. Hofhaus and Attardi (50, 51) investigated characteristics of human cell lines lacking the ND4/NuoM subunit (C4T) and the ND5/NuoL subunit (C9T). In C4T, the other mitochondrial DNA-encoded subunits failed to assemble, and there was a complete loss of NADH-quinone reductase activity. C9T showed a decreased efficiency or a reduced stability of the mitochondrial DNA-encoded subunits, and their mitochondria also exhibited little NADH-quinone reductase activity. These data seem to support our results of the NuoL-KO mutant.

Steimle *et al.* (28) reported that overexpressed NDH-1 isolated from NuoL knock-out mutant of *E. coli* displayed 80% of piericidin-sensitive NADH-DB reductase activity compared with that of the wild type. The membrane preparations of this mutant showed approximately twice the NADH-$K_3Fe(CN)_6$ reductase activity as that of the wild type. Interestingly, EPR signals of their NuoL knock-out mutant were consistent with those of the wild type. The seemingly contradicting data between theirs and ours could be explained by the difference in the experimental approach. We introduce mutations directly in the *E. coli* chromosome assuring a unique copy of the mutated gene and thus avoiding any risk of extra copies of the wild type gene.

Interestingly, the truncation of the NuoM subunit at its C terminus by exclusion of the last TM14 helix resulted in defects of subunit assembly. The ctNuoM mutants in which NuoM was truncated at the last periplasmic segment did not show notable differences in the assembly of NDH-1 when compared with the wild type. Similarly, the electron transfer activities and the proton pump activities were severely affected only in those ctNuoM mutants that were devoid of TM14. In the ctNuoM mutants lacking TM14, neither NuoM nor NuoL was detected in the membranes, whereas other subunits studied are present in the membranes to an extent similar to the wild type. The data suggest that deficiency of NuoM and/or NuoL contributed to incomplete, or lack of, NDH-1 assembly.

Furthermore, none of the ctNuoL mutants lacking the HL helix showed correct NDH-1 assembly when analyzed by BN-PAGE. Similar results were obtained even when the seven C-terminal residues of the NuoL TM16 were eliminated. The assembly of NDH-1 remained unaffected only in two mutants, ctNuoL-V611STOP and -L612STOP, in which the NuoL subunit was truncated, respectively, at the second and third residues from the C terminus. It is remarkable that, after the elimination of only seven residues of the NuoL subunit, NuoL was not detectable in the membrane, thereby causing incomplete assembly or misassembly of the whole complex. In contrast, the ctNuoL truncation mutants scarcely affected the NuoM content in the membranes. Therefore, absence of NuoL seems to trigger NDH-1 disassembly of not only ctNuoL-G488STOP,

-T517STOP, -W593STOP, A607STOP, -ΔV519-K581, but also ctNuoM-M467STOP, -G459STOP. In all probability, the null electron transfer activity seen in the case of the ctNuoL mutants that lacked the HL helix is due to the underlying structural instability and/or the inability of subunit assembly generated by very short arm for TM16 to reach its insertion site. If that is the case, it might be speculated that the region from Ala^{607} to Met^{610} in TM16 plays a key role in the NDH-1 assembly. This hypothesis should be tested in the future. In accordance with their deficiency in electron transfer activities, these ctNuoL mutants did not show capacity to generate membrane potential or proton pump activity.

The current results indicated that the extra stretch TM15-HL-TM16 in NuoL and TM14 in NuoM are essential for NDH-1 assembly and its energy-transducing activities. In contrast, three C-terminal residues of TM16 in NuoL and 25 C-terminal residues of NuoM are not required for the active NDH-1 assembly. These mapping of NDH-1 is useful in designing experimental strategy of NDH-1 to clarify structure/function of this enzyme. At the present time, NDH-1 studies tended to focus on highly conserved residues. However, on the basis of the three-dimensional structural model of NDH-1, we have recognized importance to investigate the regions without primary sequence similarity (*e.g.* secondary structural similar region). For this purpose, truncation mutants are very useful. In fact, it has been successful to clarify function of γ-subunit (so-called coiled-coil subunit) of ATP synthase (52, 53). Therefore, it is a prerequisite to study regions with low sequence similarity. This is a first report concerning NDH-1.

In conclusion, the current results point toward a possible function of the C-terminal regions of NuoM and NuoL in maintaining the stability and structure of the NDH-1. The lack of correct NDH-1 assembly and activity observed in the ctNuoL mutants analyzed in this work suggest that the structural set composed of TM15, HL helix, and the TM16 could work like rope anchor machinery by attaching the distal NuoL subunit with the rest of the membrane domain subunits and in addition, by joining the NuoL, NuoM, and NuoN subunits together, thus increasing the stability of the membrane arm subunits of NDH-1. On the other hand, considering the results of ctNuoM mutants, we cannot disregard the possibility that the truncation/elimination of the C terminus of NuoL produces a misfolded NuoL subunit, which results in an incorrect integration in the membrane and/or the whole NDH-1 complex, and thus affects its activity and assembly.

Acknowledgments—We thank Drs. Mathieu Marella and Gaurav Patki for discussion and Dr. Jennifer Barber-Singh for critical reading of the manuscript.

REFERENCES

1. Carroll, J., Fearnley, I. M., Shannon, R. J., Hirst, J., and Walker, J. E. (2003) *Mol. Cell Proteomics* **2,** 117–126
2. Carroll, J., Fearnley, I. M., Skehel, J. M., Shannon, R. J., Hirst, J., and Walker, J. E. (2006) *J. Biol. Chem.* **281,** 32724–32727
3. Lu, J., Sharma, L. K., and Bai, Y. (2009) *Cell Res.* **19,** 802–815
4. Sharma, L. K., Lu, J., and Bai, Y. (2009) *Curr. Med. Chem.* **16,** 1266–1277
5. Janssen, R. J., Nijtmans, L. G., van den Heuvel, L. P., and Smeitink, J. A. (2006) *J. Inherit. Metab. Dis.* **29,** 499–515
6. Yagi, T., Yano, T., Di Bernardo, S., and Matsuno-Yagi, A. (1998) *Biochim. Biophys. Acta* **1364,** 125–133
7. Efremov, R. G., Baradaran, R., and Sazanov, L. A. (2010) *Nature* **465,** 441–445
8. Yagi, T., and Matsuno-Yagi, A. (2003) *Biochemistry* **42,** 2266–2274
9. Hinchliffe, P., Carroll, J., and Sazanov, L. A. (2006) *Biochemistry* **45,** 4413–4420
10. Guénebaut, V., Schlitt, A., Weiss, H., Leonard, K., and Friedrich, T. (1998) *J. Mol. Biol.* **276,** 105–112
11. Yagi, T., and Dinh, T. M. (1990) *Biochemistry* **29,** 5515–5520
12. Yano, T., and Yagi, T. (1999) *J. Biol. Chem.* **274,** 28606–28611
13. Berrisford, J. M., and Sazanov, L. A. (2009) *J. Biol. Chem.* **284,** 29773–29783
14. Hinchliffe, P., and Sazanov, L. A. (2005) *Science* **309,** 771–774
15. Yakovlev, G., Reda, T., and Hirst, J. (2007) *Proc. Natl. Acad. Sci. U.S.A.* **104,** 12720–12725
16. Ohnishi, T., and Nakamaru-Ogiso, E. (2008) *Biochim. Biophys. Acta* **1777,** 703–710
17. Leonard, K., Haiker, H., and Weiss, H. (1987) *J. Mol. Biol.* **194,** 277–286
18. Peng, G., Fritzsch, G., Zickermann, V., Schägger, H., Mentele, R., Lottspeich, F., Bostina, M., Radermacher, M., Huber, R., Stetter, K. O., and Michel, H. (2003) *Biochemistry* **42,** 3032–3039
19. Radermacher, M., Ruiz, T., Clason, T., Benjamin, S., Brandt, U., and Zickermann, V. (2006) *J. Struct. Biol.* **154,** 269–279
20. Morgan, D. J., and Sazanov, L. A. (2008) *Biochim. Biophys. Acta* **1777,** 711–718
21. Mamedova, A. A., Holt, P. J., Carroll, J., and Sazanov, L. A. (2004) *J. Biol. Chem.* **279,** 23830–23836
22. Friedrich, T. (2001) *J. Bioenerg. Biomembr.* **33,** 169–177
23. Nakamaru-Ogiso, E., Sakamoto, K., Matsuno-Yagi, A., Miyoshi, H., and Yagi, T. (2003) *Biochemistry* **42,** 746–754
24. Nakamaru-Ogiso, E., Seo, B. B., Yagi, T., and Matsuno-Yagi, A. (2003) *FEBS Lett.* **549,** 43–46
25. Nakamaru-Ogiso, E., Kao, M. C., Chen, H., Sinha, S. C., Yagi, T., and Ohnishi, T. (2010) *J. Biol. Chem.* **285,** 39070–39078
26. Sinha, P. K., Castro-Guerrero, N., Matsuno-Yagi, A., Yagi, T., and Torres-Bacete, J. (2009) *Curr. Top. Biochem. Res.* **11,** 79–90
27. Hunte, C., Zickermann, V., and Brandt, U. (2010) *Science* **329,** 448–451
28. Steimle, S., Bajzath, C., Dörner, K., Schulte, M., Bothe, V., and Friedrich, T. (2011) *Biochemistry* **50,** 3386–3393
29. Nakamaru-Ogiso, E., Yano, T., Yagi, T., and Ohnishi, T. (2005) *J. Biol. Chem.* **280,** 301–307
30. Takano, S., Yano, T., and Yagi, T. (1996) *Biochemistry* **35,** 9120–9127
31. Torres-Bacete, J., Nakamaru-Ogiso, E., Matsuno-Yagi, A., and Yagi, T. (2007) *J. Biol. Chem.* **282,** 36914–36922
32. Link, A. J., Phillips, D., and Church, G. M. (1997) *J. Bacteriol.* **179,** 6228–6237
33. Kao, M. C., Di Bernardo, S., Nakamaru-Ogiso, E., Miyoshi, H., Matsuno-Yagi, A., and Yagi, T. (2005) *Biochemistry* **44,** 3562–3571
34. Kao, M. C., Nakamaru-Ogiso, E., Matsuno-Yagi, A., and Yagi, T. (2005) *Biochemistry* **44,** 9545–9554
35. Kao, M. C., Di Bernardo, S., Perego, M., Nakamaru-Ogiso, E., Matsuno-Yagi, A., and Yagi, T. (2004) *J. Biol. Chem.* **279,** 32360–32366
36. Castro-Guerrero, N., Sinha, P. K., Torres-Bacete, J., Matsuno-Yagi, A., and Yagi, T. (2010) *Biochemistry* **49,** 10072–10080
37. Yagi, T. (1986) *Arch. Biochem. Biophys.* **250,** 302–311
38. Yano, T., Sled', V. D., Ohnishi, T., and Yagi, T. (1996) *J. Biol. Chem.* **271,** 5907–5913
39. Ghelli, A., Benelli, B., and Esposti, M. D. (1997) *J. Biochem.* **121,** 746–755
40. Amarneh, B., and Vik, S. B. (2003) *Biochemistry* **42,** 4800–4808
41. Matsushita, K., Ohnishi, T., and Kaback, H. R. (1987) *Biochemistry* **26,** 7732–7737
42. Sinha, P. K., Torres-Bacete, J., Nakamaru-Ogiso, E., Castro-Guerrero, N., Matsuno-Yagi, A., and Yagi, T. (2009) *J. Biol. Chem.* **284,** 9814–9823
43. Holt, P. J., Morgan, D. J., and Sazanov, L. A. (2003) *J. Biol. Chem.* **278,** 43114–43120
44. Torres-Bacete, J., Sinha, P. K., Castro-Guerrero, N., Matsuno-Yagi, A., and

Yagi, T. (2009) *J. Biol. Chem.* **284,** 33062–33069
45. Dupuis, A., Darrouzet, E., Duborjal, H., Pierrard, B., Chevallet, M., van Belzen, R., Albracht, S. P., and Lunardi, J. (1998) *Mol. Microbiol.* **28,** 531–541
46. Dupuis, A., Peinnequin, A., Darrouzet, E., and Lunardi, J. (1997) *FEMS Microbiol. Lett.* **148,** 107–114
47. Morino, M., Natsui, S., Swartz, T. H., Krulwich, T. A., and Ito, M. (2008) *J. Bacteriol.* **190,** 4162–4172
48. Ito, M., Guffanti, A. A., Wang, W., and Krulwich, T. A. (2000) *J. Bacteriol.* **182,** 5663–5670
49. Moparthi, V. K., Kumar, B., Mathiesen, C., and Hägerhäll, C. (2011) *Biochim. Biophys. Acta* **1807,** 427–436
50. Hofhaus, G., and Attardi, G. (1993) *EMBO J.* **12,** 3043–3048
51. Hofhaus, G., and Attardi, G. (1995) *Mol. Cell. Biol.* **15,** 964–974
52. Hossain, M. D., Furuike, S., Maki, Y., Adachi, K., Suzuki, T., Kohori, A., Itoh, H., Yoshida, M., and Kinosita, K., Jr. (2008) *Biophys. J.* **95,** 4837–4844
53. Furuike, S., Hossain, M. D., Maki, Y., Adachi, K., Suzuki, T., Kohori, A., Itoh, H., Yoshida, M., and Kinosita, K., Jr. (2008) *Science* **319,** 955–958